Learning Complete Protein Representation by Deep Coupling of Sequence and Structure

Bozhen Hu

Westlake University hubozhen@westlake.edu.cn

Jun Xia

Westlake University xiajun@westlake.edu.cn

Yufei Huang

Westlake University huangyufei@westlake.edu.cn

Yue Liu

National University of Defense Technology yueliu19990731@163.com

Cheng Tan

Westlake University tancheng@westlake.edu.cn

Jiangbin Zheng

Westlake University zhengjiangbin@westlake.edu.cn

Lirong Wu

Westlake University wulirong@westlake.edu.cn

Yongjie Xu

Westlake University xuyongjie@westlake.edu.cn

Stan Z. Li*

Westlake University stan.zq.li@westlake.edu.cn

Abstract

Learning effective representations is crucial for understanding proteins and their biological functions. Recent advancements in language models and graph neural networks have enabled protein models to leverage primary or tertiary structure information to learn representations. However, the lack of practical methods to deeply co-model the relationships between protein sequences and structures has led to suboptimal embeddings. In this work, we propose CoupleNet, a network that couples protein sequence and structure to obtain informative protein representations. CoupleNet incorporates multiple levels of features in proteins, including the residue identities and positions for sequences, as well as geometric representations for tertiary structures. We construct two types of graphs to model the extracted sequential features and structural geometries, achieving completeness on these graphs, respectively, and perform convolution on nodes and edges simultaneously to obtain superior embeddings. Experimental results on a range of tasks, such as protein fold classification and function prediction, demonstrate that our proposed model outperforms the state-of-the-art methods by large margins.

1 Introduction

Proteins are the fundamental building blocks of life and play essential roles in a diversity of applications, from therapeutics to materials. They are composed of 20 different basic amino acids, which are lined by peptide bonds and form a sequence. The one-dimensional (1D) sequence of a

Preprint. Under review.

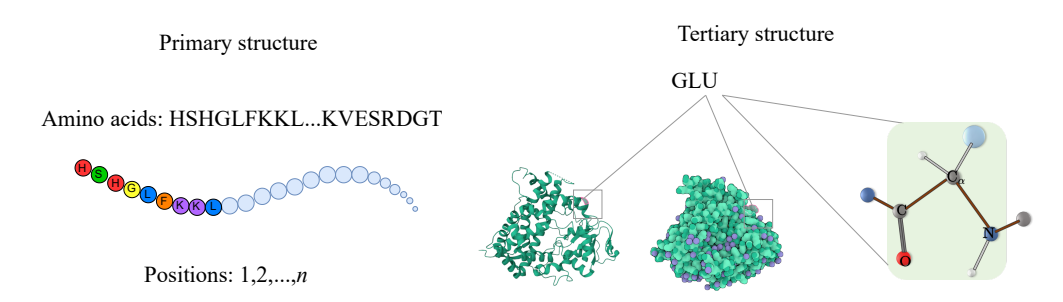


Figure 1: Illustration of the protein sequence and structure. 1) The primary structure comprises n amino acids. 2) The tertiary structure with atom arrangement in Euclidean space is presented, where each atom has a specific 3D coordinate. Amino acids have fixed backbone atoms (C_{α}, C, N, O) and side-chain atoms that vary depending on the residue types. GLU: Glutamic acid. Complete geometries can be obtained based on these coordinates. The sequence and structure provide different information types and data categories.

protein determines its structure, which in turn determines its biochemical function [40]. Due to recent progress in protein sequencing [34], massive numbers of protein sequences are now available. For example, the UniProt [3] database contains over 200 million protein sequences with annotations, *e.g.*, gene ontology (GO) terms, similar proteins, family and domains. Notably, the development of large-scale language models (LMs) in natural language processing has substantially benefited protein research owing to similarities between human language and protein sequences [16, 27]. For instance, models like ProtTrans [14] and ESM-series [39, 33] in learning protein representations have proven successful utility of pre-training protein LMs with self-supervision to process protein sequences.

Thanks to the recent significant progress made by AlphaFold2 [30] in three-dimensional (3D) structure prediction, a large number of protein structures from their sequence data are now made available. The latest release of AlphaFold protein structure database [43] provides broad coverage of UniProt [3]. Recently proposed structure-based protein encoders become to utilize geometric features [25, 24, 53], e.g., ProNet [47] learns representations of proteins with 3D structures at different levels, like the amino acid, backbone or all-atom levels. There also exists a group of methods that build graph neural networks and LMs (LSTMs or attention models) to process sequence and structure [53, 50, 19], for example, GearNet [53] encodes sequential and spatial features by alternating node and edge message passing on protein residue graphs.

The 1D sequence and 3D structure of a protein provide different types of information, in detail, as shown in Figure 1, compared with the 1D sequential order and amino acids in peptide chains, the tertiary structure provides 3D coordinates of each atom in protein residues, which allow them to perform precise functions. Although a protein's sequence determines its structure, various works have demonstrated the effectiveness of learning from either sequence or structure [33, 25]. However, rich constraints between the sequence and structure of a protein, which may be critical for protein tasks [4], have yet to be fully explored. Most protein sequence-structure modeling methods cannot deeply integrate the information behind sequence and structure for the reason that they tend to fuse representations together, extracted from sequence and structure encoders, respectively, by message passing mechanism [8] or by simple concatenation operations.

In this work, we aim to learn protein representations by deeply coupling the protein sequences and structures. Considering the relative positions of residues in the sequence and the spatial arrangement of atoms in the Euclidean space, the proposed CoupleNet constructs two categories of graphs for them, respectively. The complete representations are obtained at the base and backbone levels on the two graphs, which are used as node and edge features to learn the final graph-level representations. Rather than concatenating sequence and structure representations, we take advantage of graph convolutions, performing node and edge convolutions simultaneously. The contributions of this paper are threefold:

• We propose a novel two-graph-based approach for representing the sequence and the 3D geometric structure of a protein, which is an effective way to guarantee completeness.

- We propose CoupleNet, a model that performs convolutions on nodes and edges of graphs to effectively integrate protein sequence and structure. This can better model the node-edge relationships and utilize the intrinsic associations between sequences and structures.
- Practically, the proposed model is verified by obtaining new state-of-the-art experimental
 results compared with current mainstream protein representation learning methods on a
 range of tasks, including protein fold classification, enzyme reaction classification, GO term
 prediction, domain prediction, and enzyme commission number prediction.

2 Related Work

Protein Representation Learning Protein representation learning has become an active and promising direction in biology, which is essential to various downstream tasks in protein science. Because of the different levels of protein structures, existing methods mainly fall into three categories: protein LMs for sequences, structure models for geometry, and hybrid methods for both of them. As proteins are sequences of amino acids, considering their similarities with human languages, UniRep [1], UDSMProt [42] and SeqVec [23] use LSTM or its variants to learn sequence representations and long-range dependencies. TAPE [37] benchmarks a group of protein models, e.g., 1D CNN, LSTM, and Transformer by various tasks. Elnaggar et al. [14] have trained six successful transformer variants on billions of amino acid sequences, like ProtBert, and ProtT5. Similarly, ESM-series [39, 38, 33] employs a transformer architecture and a masked language modeling strategy to train robust representations based on large-scale databases. Besides the protein sequence, as we have stated before, the 3D geometric structure is vital to enhance protein representations. Most methods commonly seek to encode the spatial information of protein structures by convolutional neural networks (CNNs) [11], or graph neural networks [19, 2, 29]. For instance, SPROF [7] employs distance maps to predict protein sequence profiles, and IEConv [25] introduces a convolution operator to capture all relevant structural levels of a protein. GVP-GNN [29] designs the geometric vector perceptrons (GVP) for learning both scalar and vector features in an equivariant and invariant manner, Guo et al. [21] adopt SE(3)-invariant features as the model inputs and reconstruct gradients over 3D coordinates to avoid the usage of complicated SE(3)-equivariant models. ProNet [47] learns hierarchical protein representations at multiple tertiary structure levels of granularity. Moreover, CDConv [15] proposes continuous-discrete convolution using irregular and regular approaches to model the geometry and sequence structures. Some protein learning methods model the multi-level of structures at the same time [53, 6, 15], except for the primary structure and the tertiary structure, the second refers to the 3D form of local segments of proteins (e.g., α -helix, β -strand), the quaternary is a protein multimer comprising multiple polypeptides, for example, PromtProtein [48] adopts a prompt-guided multi-task learning strategy for different protein structures with specific pre-training tasks. While previous works have attempted to combine protein sequence and structure, we focus on profoundly integrating them by specifically designing two types of graphs respectively and conducting convolutions simultaneously to learn protein representations.

Complete Message Passing Mechanism ComENet [46] proposes rotation angles and spherical coordinates to fulfil the global completeness of 3D information on molecular graphs. By incorporating these designed geometric representations into the message passing scheme [18], the complete representation for a whole 3D graph is eventually yielded [47]. Unlike these methods, we couple sequence and structure via corresponding graphs and different geometric representations to obtain completeness representations.

3 Method

3.1 Preliminaries

Notations We represent a 3D graph as $G = (\mathcal{V}, \mathcal{E}, \mathcal{P})$, where $\mathcal{V} = \{v_i\}_{i=1,\dots,n}$ and $\mathcal{E} = \{\varepsilon_{ij}\}_{i,j=1,\dots,n}$ denote the vertex and edge sets with n nodes in total, respectively, and $\mathcal{P} = \{P_i\}_{i=1,\dots,n}$ is the set of position matrices, where $P_i \in \mathbb{R}^{k_i \times 3}$ represents the position matrix for node v_i . We treat each amino acid as a graph node for a protein, then k_i depends on the number of atoms in the i-th amino acid. The node feature matrix is $X = [\mathbf{x}_i]_{i=1,\dots,n}$, where $\mathbf{x}_i \in \mathbb{R}^{d_v}$ is

the feature vector of node v_i . The edge feature matrix is $E = [e_{ij}]_{i,j=1,\dots,n}$, where $e_{ij} \in \mathbb{R}^{d_{\varepsilon}}$ is the feature vector of edge ε_{ij} . d_v and d_{ε} denote the dimensions of feature vectors \boldsymbol{x}_i and e_{ij} .

Invariance and Equivariance We consider affine transformations that preserve the distance between any two points, *i.e.*, the isometric group SE(3) in the Euclidean space. This is called the symmetry group, and it turns out that SE(3) is the special Euclidean group that includes 3D translations and the 3D rotation group SO(3) [17, 12]. The matrix form of SE(3) is provided in Appendix A.1.

Given the function $f: \mathbb{R}^m \to \mathbb{R}^{m'}$, assuming the given symmetry group G acts on \mathbb{R}^m and $\mathbb{R}^{m'}$, then f is G-equivariant if,

$$f(T_g \mathbf{x}) = S_g f(\mathbf{x}), \ \forall \mathbf{x} \in \mathbb{R}^m, g \in G$$
(1)

where T_g and S_g are the transformations. For the SE(3) group, when $m^{'}=1$, the output of f is a scalar, we have

$$f(T_q \mathbf{x}) = f(\mathbf{x}), \ \forall \mathbf{x} \in \mathbb{R}^m, q \in G$$
 (2)

thus f is SE(3)-invariant.

Complete Geometric Representations A geometric transformation $\mathcal{F}(\cdot)$ is complete if two 3D graphs $G^1 = (\mathcal{V}, \mathcal{E}, \mathcal{P}^1)$ and $G^2 = (\mathcal{V}, \mathcal{E}, \mathcal{P}^2)$, there exists $T_g \in SE(3)$ such that the representations

$$\mathcal{F}(G^1) = \mathcal{F}(G^2) \Longleftrightarrow P_i^1 = T_g(P_i^2), \text{ for } i = 1, \dots n$$
 (3)

The operation T_g would not change the 3D conformation of a 3D graph [46]. Positions can generate geometric representations, which can also be recovered from them.

Message Passing Paradigm Message passing mechanism is mainly applied in graph convolutional networks (GCNs) [32], which follows an iterative scheme of updating node representations based on the feature aggregation from nearby nodes.

$$\mathbf{h}_{i}^{(0)} = \text{BN}\left(\text{FC}\left(\mathbf{x}_{i}\right)\right),$$

$$\mathbf{u}_{i}^{(l)} = f_{\text{Agg}}^{(l)}(\mathbf{h}_{j}^{(l-1)}|v_{j} \in \mathcal{N}(v_{i})),$$

$$\mathbf{h}_{i}^{(l)} = f_{\text{Update}}^{(l)}(\mathbf{h}_{j}^{(l-1)}, \mathbf{u}_{i}^{(l)})$$

$$(4)$$

where $FC(\cdot)$ and $BN(\cdot)$ mean the linear transformation and batch normalization respectively. $\mathcal{N}(v_i)$ denotes the neighbours of node v_i . $f_{Agg}^{(l)}$ and $f_{Update}^{(l)}$ are aggregation and transformation functions at the l-th layer, which are permutation invariant and equivariant of node representations.

3.2 Sequence-Structure Graph Construction

Specifically, we represent each amino acid as a node, considering the residue types and their positions $i=1,2,\cdots,n$ (See Figure 1) in the sequence, we define the sequential graph primarily on the sequence, if $\|i-j\| < l$, the edge ε_{ij} exists, where l is a hyperparameter. Besides the sequential graph, we predefine a radius r, and build the radius graph, and there exists an edge between node v_i and v_j if $\|P_{i,\mathrm{C}\alpha}-P_{j,\mathrm{C}\alpha}\|< r$, where $P_{i,\mathrm{C}\alpha}$ denotes the 3D position of C_α in the i-th residue.

Firstly, we design a base approach called CoupleNet_{aa} that only uses the C_{α} positions of the structures. Inspired by Ingraham *et al.* [28], we construct a local coordinate system (LCS) for each residue, as shown in Figure 2.

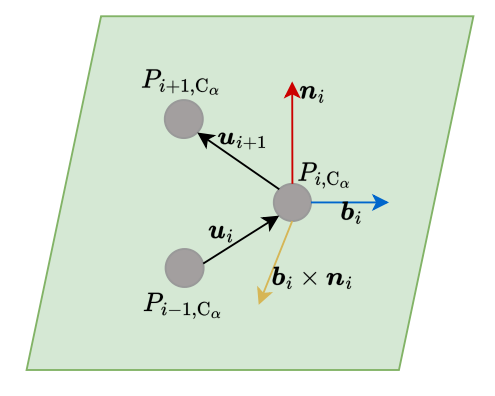


Figure 2: The local coordinate system.

$$Q_i = [b_i \quad n_i \quad b_i \times n_i] \tag{5}$$

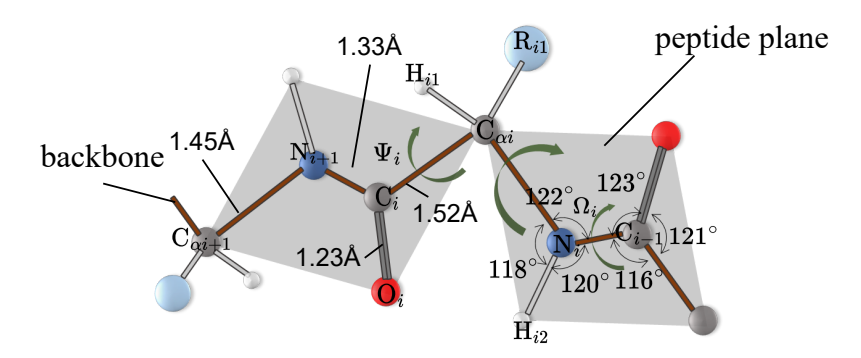


Figure 3: The polypeptide chain depicting the characteristic backbone bond lengths, angles, and torsion angles $(\Psi_i, \Phi_i, \Omega_i)$. The planar peptide groups are denoted as shaded gray regions, indicating that the peptide plane differs from the geometric plane calculated based on the 3D positions.

where $u_i = \frac{P_{i,C\alpha} - P_{i-1,C\alpha}}{\|P_{i,C\alpha} - P_{i-1,C\alpha}\|}, b_i = \frac{u_i - u_{i+1}}{\|u_i - u_{i+1}\|}, n_i = \frac{u_i \times u_{i+1}}{\|u_i \times u_{i+1}\|}$. Then we can get the geometric representations at the base level of a protein 3D graph,

$$\mathcal{F}(G)_{ij,aa} = (\|P_{i,C\alpha} - P_{j,C\alpha}\|, \mathbf{Q}_i^T \cdot \frac{P_{i,C\alpha} - P_{j,C\alpha}}{\|P_{i,C\alpha} - P_{j,C\alpha}\|}, \mathbf{Q}_i^T \cdot \mathbf{Q}_j)$$

$$(6)$$

where \cdot is the matrix multiplication, this implementation is SE(3)-equivariant and obtains complete representations at the base level; as if we have Q_i , the LCS Q_j can be easily obtained by $\mathcal{F}(G)_{ij,aa}$.

For a node v_i , the node features $x_{i,aa}$ in the baseline approach is the concatenation of the one-hot embeddings of the amino acid types and the physicochemical properties of each residue, namely, a steric parameter, hydrophobicity, volume, polarizability, isoelectric point, helix probability and sheet probability [51, 22], which provide quantitative insights into the biochemical nature of each amino acid. And $\mathcal{F}(G)_{ij,aa}$ is set as edge features for CoupleNet_{aa}.

Secondly, we consider all backbone atoms C_{α}, C, N, O in CoupleNet. In detail, the peptide bond exhibits partial double-bond character due to resonance [20], indicating that the three non-hydrogen atoms comprising the bond (the carbonyl oxygen, carbonyl carbon, and amide nitrogen) are coplanar, as shown in Figure 3. There is some rotation about the connection. The $N_i-C_{\alpha i}$ and $C_{\alpha i}-C_i$ bonds, are the two bonds in the basic repeating unit of the polypeptide backbone. These single bonds allow unrestricted rotation until sterically restricted by side chains [35, 45]. Since the coordinates of C_{α} can be obtained as we have the complete representations at the base level, the coordinates of other backbone atoms based on these rigid bond lengths and angles are able to be determined with the remaining degree of the backbone torsion angles Φ_i, Ψ_i, Ω_i . The omega torsion angle around the C-N peptide bond is typically restricted to nearly 180° (trans) but can approach 0° (cis) in rare instances. Other than the bond lengths and angles presented in Figure 3, all the H bond lengths measure approximately 1 Å.

For the sequential graph, we compute the sine and cosine values of Φ_i , Ψ_i , Ω_i for each amino acid i, and use them as another part of nodes features for node v_i .

$$\boldsymbol{x}_i = \boldsymbol{x}_{i,aa} \| ((\sin \wedge \cos)(\Phi_i, \Psi_i, \Omega_i))$$
 (7)

where \parallel denotes concatenation. There is no isolated node for the designed graph, which means the backbone atoms can be determined one by one along the polypeptide chain based on the positions of C_{α} and these three backbone dihedral angles. Therefore, the existing presentations $[\mathcal{F}(G)_{ij,aa}]_{i,j=1,...,n}$ and $[\boldsymbol{x}_i]_{i=1,...,n}$ are complete at the backbone level for the sequential graph.

For the radius graph, we want to get the positions of backbone atoms in any two amino acids i and j. Inspired by trRosetta [52], the relative rotation and distance are computed including the distance $(d_{ij,C_{\beta}})$, three dihedral angles $(\omega_{ij},\theta_{ij},\theta_{ji})$ and two planar angles $(\varphi_{ij},\varphi_{ji})$, as shown in Figure 4, where $d_{ij,C_{\beta}}=d_{ji,C_{\beta}},\omega_{ij}=\omega_{ji}$, but θ and φ values depend on the order of residues. These interresidue geometries define the relative locations of the backbone atoms of two residues in all their details [52], because the torsion angles of $N_i - C_{\alpha i}$ and $C_{\alpha i} - C_i$ do not influence their positions. Therefore, these six geometries are complete for amino acids at the backbone level for the

radius graph. The graph edges contain the relative spatial information between any two neighboring amino acids $e_{ij} = \mathcal{F}(G)_{ij,aa} \| \mathcal{F}(G)_{ij,bb}$, where

$$\mathcal{F}(G)_{ij,bb} = (d_{ij,C_{\beta}}, (\sin \wedge \cos)(\omega_{ij}, \theta_{ij}, \varphi_{ij}))$$
(8)

The designed node and edge features, x_i and e_{ij} , for the sequential and radius graphs, provide a new perspective to represent protein sequences and structures. Such integration can bring better performance for the following graph-based learning tasks.

3.3 Secquice-Structure Graph Convolution

Inspired by the message passing paradigm and continuousdiscrete convolution [15], sequences and structures are encoded successfully together by convolutions. To deeply couple sequences and structures of proteins and encode them jointly, we employ convolution to embed them simultaneously, exploring their relationships to generate comprehensive and effective embeddings. Different from previous works, we innovatively construct two categories of graphs for sequence and structure and design various sequential and structural representations to achieve completeness on them at the base and backbone levels. We then convolve node and edge features with the help of the message passing mechanism.

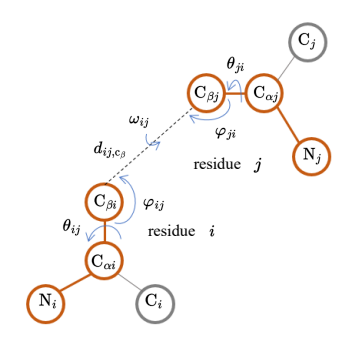


Figure 4: Interresidue geometries including angles and distances.

In order to implement convolution on nodes and edges simultaneously between sequence and structure, we set ε_{ij} to exist if the following conditions are satisfied

$$||i - j|| < l \quad \text{and} \quad ||P_{i,C\alpha} - P_{j,C\alpha}|| < r$$
 (9)

The existing node and edge feature matrices (X, E) are complete representations of a protein 3D graph to reconstruct its backbone atom positions. Compared with the equation Eq. 4, the proposed CoupleNet first apply a $FC(\cdot)$ layer and a $BN(\cdot)$ layer to the node features to obtain the initial encoded representation. Then the $f_{Agg}^{(l)}$ is applied to gather neighboring features of nodes and edges by convolution, where $\sigma(\cdot)$ is the activation function, and W is the learnable convolutional kernel matrix. We use the dropout and add a residual connection from the previous layer as $f_{Update}^{(l)}$. For the consideration that the spatial arrangement and tight positioning of specific amino acids, which may be spaced widely apart on the linear polypeptide, are necessary for proteins to operate as intended [10], l is set to be a relatively large number, see Appendix A.2 for details.

$$\boldsymbol{h}_{i}^{(0)} = BN \left(FC \left(\boldsymbol{x}_{i}\right)\right),$$

$$\boldsymbol{u}_{i}^{(l)} = \sigma \left(BN \left(\sum_{v_{j} \in \mathcal{N}\left(v_{i}\right)} W \boldsymbol{e}_{ij} \boldsymbol{h}_{j}^{(l-1)}\right),$$

$$\boldsymbol{h}_{i}^{(l)} = \boldsymbol{h}_{i}^{(l)} + Dropout(\boldsymbol{u}_{i}^{(l)})$$
(10)

3.4 Model Architecture

Building upon the sequence-structure graph convolution, we build the CoupleNet, as shown in Figure 5. The inputs to the graph are the calculated sequential and structural representations (X,E). Following the existing protein graph models [15, 25, 47], our CoupleNet employs graph pooling layers to obtain deeply encoded, graph-level representations. After pooling, due to the decrease in nodes, we increase the predefined radius r to include more neighbors. The message passing mechanism only executes on nodes for the consideration of reducing model complexity. Another reason is that representations of sequences and structures have already been coupled by equation Eq. 4. A detailed description of the model architecture is provided in Appendix A.2.

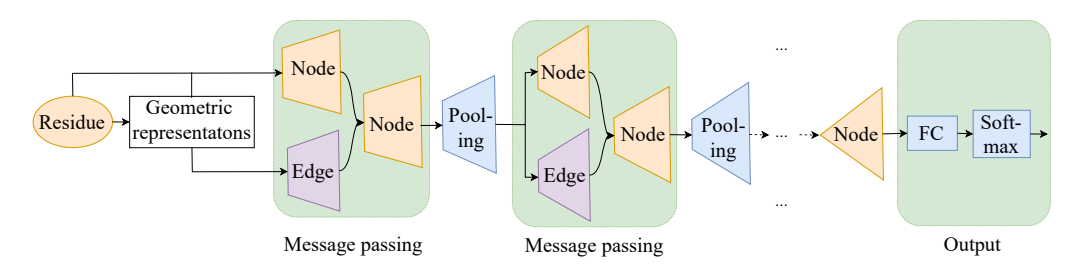


Figure 5: An illustration of CoupleNet.

4 Experiments

4.1 Datasets and Settings

The models are trained with the Adam optimizer [31] using the PyTorch and PyTorch Geometric libraries. Detailed descriptions of the datasets and experimental settings are provided in Appendix A.3. Following the tasks in IEconv [25], GearNet [53] and CDConv [15], here, we evaluate the CoupleNet on four protein tasks: protein fold classification, enzyme reaction classification, GO term prediction and enzyme commission (EC) number prediction.

Fold Classification Protein fold is to predict the fold class label given a protein, which is crucial for understanding how protein structure and protein evolution interact [26]. In total, this dataset contains 16, 712 proteins with 1, 195 fold classes. There are three test sets available, Fold: Training excludes proteins from the same superfamily. Superfamily: Training does not include proteins from the same family. Family: Proteins from the same family are included in the training.

Enzyme Reaction Classification Reaction categorization aims to predict a protein's class of enzyme-catalyzed reactions, according to all four levels of the EC number [49, 36]. Following the setting in [25], this dataset has 37, 248 proteins from 384 four-level EC numbers [5].

GO Term Prediction The goal of GO term prediction is to foretell whether a protein is related to a certain GO term. Following [19], these proteins are organized into three ontologies: molecular function (MF), biological process (BP), and cellular component (CC), which are hierarchically connected, functional classes. MF describes activities that occur at the molecular level, BP represents the larger processes, and CC describes the parts of a cell or its extracellular environment [3].

EC Number Prediction This task seeks to predict the 538 EC numbers from the third level and fourth levels of different proteins [19], which describe their catalysis of biochemical reactions.

4.2 Baselines

We compare our proposed method with existing protein representation learning methods, which are classified into three categories based on their inputs, which could be a sequence (amino acid sequence), 3D structure or both sequence and structure. 1) Sequence-based encoders, including CNN [41], ResNet [37], LSTM [37] and Transformer [37]. 2) Structure-based methods (GCN [32], GAT [44], 3DCNN_MQA [11], IEConv (atom level) [25]). 3) Sequence-structure based models, *e.g.*, GVP [29], ProNet [47], GearNet [53], CDConv [15], *etc.* GearNet-IEConv and GearNetEdge-IEConv [53] add the IEConv layer based on GearNet, which is found important in fold classification.

4.3 Resluts of Fold and Reaction Classification.

Table 1 provides the comparisons on the fold and enzyme reaction classification. The results are reported in terms of accuracy (%) for these two tasks. From this table, we can see that the proposed model CoupleNet achieves the best performance across all four test sets on the fold and enzyme reaction classification compared with recent state-of-the-art methods. Especially on the Fold and SuperFamily test sets, CoupleNet improves the results by about 4%, showing that CoupleNet is proficient at learning the mapping between protein sequences, structures and functions. Moreover,

Table 1: Accuracy (%) on fold classification and enzyme reaction classification. [*] means the results are taken from [15]. The best and suboptimal results are shown in bold and underline.

Input	Method		Enzyme		
imput	Nemou	Fold	SuperFamily	Family	Reaction
	CNN [41]*	11.3	13.4	53.4	51.7
Caguanaa	ResNet [37]*	10.1	7.21	23.5	24.1
Sequence	LSTM [37]*	6.41	4.33	18.1	11.0
	Transformer [37]*	9.22	8.81	40.4	26.6
	GCN [32]*	16.8	21.3	82.8	67.3
Structure	GAT [44]*	12.4	16.5	72.7	55.6
Structure	3DCNN_MQA [11]*	31.6	45.4	92.5	72.2
	IEConv (atom level) [25]*	45.0	69.7	98.9	87.2
	GraphQA [2]*	23.7	32.5	84.4	60.8
	GVP [29]*	16.0	22.5	83.8	65.5
	ProNet-Amino Acid [47]	51.5	69.9	99.0	86.0
	ProNet-Backbone [47]	52.7	70.3	99.3	86.4
	ProNet-All-Atom [47]	52.1	69.0	99.0	85.6
Caguanaa Ctmiatura	IEConv (residue level) [25]*	47.6	70.2	99.2	87.2
Sequence-Structure	GearNet [53]	28.4	42.6	95.3	79.4
	GearNet-IEConv [53]	42.3	64.1	99.1	83.7
	GearNet-Edge [53]	44.0	66.7	99.1	86.6
	GearNet-Edge-IEConv [53]	48.3	70.3	99.5	85.3
	CDConv [15]	<u>56.7</u>	<u>77.7</u>	<u>99.6</u>	<u>88.5</u>
	CoupleNet (Proposed)	60.6	82.1	99.7	89.0

CDConv [15] ranks second among these methods, both CDConv and our method are implemented by sequence-structure convolution. This phenomenon illustrates that deeply coupling sequences and structures of proteins is conducive to learning better protein embeddings. And our proposed CoupleNet model utilizes complete geometric representations and the specially designed message passing mechanism, achieving new state-of-the-art results.

4.4 Results of GO Term and EC Prediction

We follow the split method in [19, 53] to guarantee that the test set only comprises PDB chains with sequence identity no higher than 95% to the training set for GO term and EC number prediction. Table 2 compares different protein modeling methods on GO term prediction and EC number prediction. The results are reported in terms of F_{max}, which considers both precision and recall for evaluation, the equation of $F_{\rm max}$ is provided in Appendix A.4. The proposed model, CoupleNet yields the highest F_{max} across these four test sets of two tasks, outperforming other state-of-the-art models. This indicates CoupleNet can effectively predict the functions, locations, and enzymatic activities of proteins. These results once again illustrate the

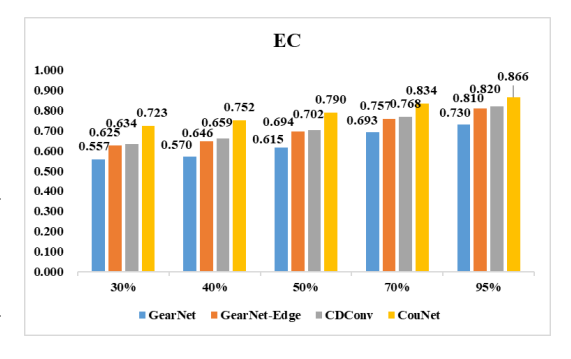


Figure 6: $F_{\rm max}$ on EC number prediction under different cutoffs.

importance of deeply coupled sequences and structures. The improvements of CoupleNet over the suboptimal CDConv [15] model indicate the advanced modeling power of CoupleNet.

We employ different cutoff splits following [19, 15], which means that the proteins in the test set are divided into groups that have, respectively, 30%, 40%, 50%, 70%, and 95% similarity to the training set for GO term and EC number prediction, as shown in Figure 6 and Appendix A.5. From

Table 2: $F_{\rm max}$ on GO term and EC number prediction. [*] means the results are taken from [15]. The best and suboptimal results are shown in bold and underline.

Category	Method	GO-BP	GO-MF	GO-CC	EC
	CNN [41]*	0.244	0.354	0.287	0.545
Caguanaa	ResNet [37]*	0.280	0.405	0.304	0.605
Sequence	LSTM [37]*	0.225	0.321	0.283	0.425
	Transformer [37]*	0.264	0.211	0.405	0.238
	GCN [32]*	0.252	0.195	0.329	0.320
Structure	GAT [44]*	0.284	0.317	0.385	0.368
	3DCNN_MQA [11]*	0.240	0.147	0.305	0.077
	GraphQA [2]*	0.308	0.329	0.413	0.509
	GVP [29]*	0.326	0.426	0.420	0.489
	IEConv (residue level) [25]*	0.421	0.624	0.431	-
Caguanaa Ctmuatuma	GearNet [53]	0.356	0.503	0.414	0.730
Sequence-Structure	GearNet-IEConv [53]	0.381	0.563	0.422	0.800
	GearNet-Edge [53]	0.403	0.580	0.450	0.810
	GearNet-Edge-IEConv [53]	0.400	0.581	0.430	0.810
	CDConv [15]	0.453	0.654	0.479	0.820
	CoupleNet (Proposed)	0.467	0.669	0.494	0.866

Table 3: Ablation of our proposed method

Method	Fold Classification		Enzyme	GO		EC		
Method	Fold	Superfamily	Family	Reaction	BP	MF	CC	EC
CoupleNet	60.6	82.1	99.7	89.0	0.467	0.669	0.494	0.866
$CoupleNet_{aa}$	57.8	78.7	99.6	88.6	0.458	0.660	0.484	0.851
w/o Φ, Ψ, Ω	60.3	81.3	99.6	88.7	0.463	0.666	0.490	0.862
w/o $d, \omega, \theta, \varphi$	60.4	81.5	99.7	88.9	0.461	0.666	0.488	0.864

Figure 6, we can see that our proposed model CoupleNet achieves the highest $F_{\rm max}$ scores across all cutoffs, especially when the cutoffs are at 30% to 50%. There is a larger margin compared with GearNet, GearNet-Edge [53] and CDConv [15]. This demonstrates that CoupleNet, which utilizes complete geometric representations, is more robust, especially when there is a low similarity between the training and test sets.

4.5 Ablation Study

Table 3 presents an ablation study of the proposed CoupleNet model on the four protein tasks. We examined the impact of removing the backbone torsion angles (w/o Φ, Ψ, Ω) and removing the interresidue geometric structure representations (w/o $d_{C_\beta}, \omega, \theta, \varphi$). The former is designed for the sequential graph, and the latter is for the radius graph to achieve completeness at the protein backbone level. However, we combine the two types of graphs together to enhance the relationships between sequence and structure. From Table 3, we can also find that these complete geometries provide complementary information to amino acid position features, with one of their removals leading to minor performance drops for the reason that they both provide complete geometries from different perspectives. Removing Φ, Ψ, Ω causes larger performance degradation compared with removing $d_{C_\beta}, \omega, \theta, \varphi$. Such comparisons indicate that the backbone dihedral angles may have more effects on learning protein representations in these experimental settings. CoupleNet_{aa} is a base model that only adopts the C_α position of protein structures. Compared with CoupleNet_{aa}, CoupleNet achieves significant improvements on the four tasks, demonstrating the importance of complete structural representations at the backbone level in learning protein embeddings.

5 Conclusions and Limitations

In this work, we propose CoupleNet, a novel protein representation learning method that deeply fuses protein sequences and multi-level structures by conducting convolution on graph nodes and edges simultaneously. We design the sequential graph and the radius graph, achieving completeness on them at different protein structure levels. Our approach achieves new state-of-the-art results on the protein tasks, which demonstrates the superiority our the proposed method. A limitation is that the detailed inter-relationships between sequence and structures remain to be explored and uncovered. We leave such research for future work.

While our model can enable advanced protein analyses and provide effective representations, there may exist broader impacts and harmful activities. The representations could potentially be misused, *e.g.*, for designing harmful molecules or proteins.

References

- [1] Ethan C. Alley et al. "Unified rational protein engineering with sequence-based deep representation learning". In: *Nature Methods* (2019).
- [2] Federico Baldassarre et al. "GraphQA: protein model quality assessment using graph convolutional networks." In: *Bioinformatics* (2020).
- [3] Alex Bateman. "UniProt: A worldwide hub of protein knowledge". In: *Nucleic Acids Research* (2019).
- [4] Tristan Bepler and Bonnie Berger. "Learning the protein language: Evolution, structure, and function". In: *Cell systems* 12.6 (2021), pp. 654–669.
- [5] Helen M Berman et al. "The protein data bank". In: *Nucleic acids research* 28.1 (2000), pp. 235–242.
- [6] Can Chen et al. "Structure-aware protein self-supervised learning". In: *Bioinformatics* 39.4 (2023), btad189.
- [7] Sheng Chen et al. "To Improve Protein Sequence Profile Prediction through Image Captioning on Pairwise Residue Distance Map". In: *Journal of Chemical Information and Modeling* (2020).
- [8] Yihong Chen et al. "Refactor gnns: Revisiting factorisation-based models from a message-passing perspective". In: *Advances in Neural Information Processing Systems* 35 (2022), pp. 16138–16150.
- [9] G Marius Clore and Angela M Gronenborn. "NMR structure determination of proteins and protein complexes larger than 20 kDa". In: *Current opinion in chemical biology* 2.5 (1998), pp. 564–570.
- [10] Srinivasan Damodaran. "Amino acids, peptides and proteins". In: Fennema's food chemistry 4 (2008), pp. 425–439.
- [11] Georgy Derevyanko et al. "Deep convolutional networks for quality assessment of protein folds". In: *Bioinformatics* 34.23 (2018), pp. 4046–4053.
- [12] Weitao Du et al. "SE (3) Equivariant Graph Neural Networks with Complete Local Frames". In: *International Conference on Machine Learning*. PMLR. 2022, pp. 5583–5608.
- [13] Arun Kumar Dubey and Vanita Jain. "Comparative study of convolution neural network's relu and leaky-relu activation functions". In: *Applications of Computing, Automation and Wireless Systems in Electrical Engineering: Proceedings of MARC 2018.* Springer. 2019, pp. 873–880.
- [14] Ahmed Elnaggar et al. "ProtTrans: Towards Cracking the Language of Lifes Code Through Self-Supervised Deep Learning and High Performance Computing". In: *IEEE Transactions on Pattern Analysis and Machine Intelligence* (2021).
- [15] Hehe Fan et al. "Continuous-Discrete Convolution for Geometry-Sequence Modeling in Proteins". In: *The Eleventh International Conference on Learning Representations*. 2023.
- [16] Noelia Ferruz and Birte Höcker. "Controllable protein design with language models". In: *Nature Machine Intelligence* (2022), pp. 1–12.
- [17] Fabian Fuchs et al. "Se (3)-transformers: 3d roto-translation equivariant attention networks". In: *Advances in Neural Information Processing Systems* 33 (2020), pp. 1970–1981.
- [18] Justin Gilmer et al. "Neural message passing for quantum chemistry". In: *International conference on machine learning*. PMLR. 2017, pp. 1263–1272.
- [19] Vladimir Gligorijević et al. "Structure-based protein function prediction using graph convolutional networks". In: *Nature communications* 12.1 (2021), p. 3168.
- [20] ER HARD GROSS and JOHANNES MEIENHOFER. "The Peptide Bond". In: *Major Methods of Peptide Bond Formation: The Peptides Analysis, Synthesis, Biology, Vol. 1* 1 (2014), p. 1.
- [21] Yuzhi Guo et al. "Self-supervised pre-training for protein embeddings using tertiary structures". In: Proceedings of the AAAI Conference on Artificial Intelligence. Vol. 36. 6. 2022, pp. 6801–6809
- [22] Jack Hanson et al. "Improving prediction of protein secondary structure, backbone angles, solvent accessibility and contact numbers by using predicted contact maps and an ensemble of recurrent and residual convolutional neural networks". In: *Bioinformatics* 35.14 (2019), pp. 2403–2410.
- [23] Michael Heinzinger et al. "Modeling the language of life Deep Learning Protein Sequences". In: bioRxiv (2019).

- [24] Pedro Hermosilla and Timo Ropinski. "Contrastive representation learning for 3d protein structures". In: *arXiv preprint arXiv:2205.15675* (2022).
- [25] Pedro Hermosilla et al. "Intrinsic-Extrinsic Convolution and Pooling for Learning on 3D Protein Structures". In: *International Conference on Learning Representations* (2021).
- [26] Jie Hou, Badri Adhikari, and Jianlin Cheng. "DeepSF: deep convolutional neural network for mapping protein sequences to folds". In: *Bioinformatics* 34.8 (2018), pp. 1295–1303.
- [27] Bozhen Hu et al. "Protein Language Models and Structure Prediction: Connection and Progression". In: *arXiv preprint arXiv:2211.16742* (2022).
- [28] John Ingraham et al. "Generative models for graph-based protein design". In: *Advances in neural information processing systems* 32 (2019).
- [29] Bowen Jing et al. "Learning from Protein Structure with Geometric Vector Perceptrons". In: *Learning* (2020).
- [30] John Jumper et al. "Highly accurate protein structure prediction with AlphaFold". In: *Nature* 596.7873 (2021), pp. 583–589.
- [31] Diederik P Kingma and Jimmy Ba. "Adam: A method for stochastic optimization". In: *arXiv* preprint arXiv:1412.6980 (2014).
- [32] Thomas N Kipf and Max Welling. "Semi-supervised classification with graph convolutional networks". In: *arXiv preprint arXiv:1609.02907* (2016).
- [33] Zeming Lin et al. "Language models of protein sequences at the scale of evolution enable accurate structure prediction". In: *BioRxiv* (2022).
- [34] Bin Ma. "Novor: real-time peptide de novo sequencing software." In: *Journal of the American Society for Mass Spectrometry* (2015).
- [35] David L Nelson, Albert L Lehninger, and Michael M Cox. Lehninger principles of biochemistry. Macmillan, 2008.
- [36] Marina V Omelchenko et al. "Non-homologous isofunctional enzymes: a systematic analysis of alternative solutions in enzyme evolution". In: *Biology direct* 5 (2010), pp. 1–20.
- [37] Roshan Rao et al. "Evaluating protein transfer learning with TAPE". In: *Advances in neural information processing systems* 32 (2019).
- [38] Roshan M Rao et al. "MSA transformer". In: *International Conference on Machine Learning*. PMLR. 2021, pp. 8844–8856.
- [39] Alexander Rives et al. "Biological Structure and Function Emerge from Scaling Unsupervised Learning to 250 Million Protein Sequences". In: *Proceedings of the National Academy of Sciences of the United States of America* (2019).
- [40] Andrew W Senior et al. "Improved protein structure prediction using potentials from deep learning". In: *Nature* 577.7792 (2020), pp. 706–710.
- [41] Amir Shanehsazzadeh, David Belanger, and David Dohan. "Is transfer learning necessary for protein landscape prediction?" In: *arXiv preprint arXiv:2011.03443* (2020).
- [42] Nils Strodthoff et al. "UDSMProt: universal deep sequence models for protein classification". In: *Bioinformatics* 36.8 (Jan. 2020), pp. 2401–2409. ISSN: 1367-4803. DOI: 10.1093/bioinformatics/btaa003.
- [43] Mihaly Varadi et al. "AlphaFold Protein Structure Database: massively expanding the structural coverage of protein-sequence space with high-accuracy models". In: *Nucleic acids research* 50.D1 (2022), pp. D439–D444.
- [44] Petar Velickovic et al. "Graph attention networks". In: stat 1050.20 (2017), pp. 10–48550.
- [45] K Peter C Vollhardt and Neil E Schore. *Organic chemistry: structure and function*. Macmillan, 2003.
- [46] Limei Wang et al. "ComENet: Towards Complete and Efficient Message Passing for 3D Molecular Graphs". In: *arXiv preprint arXiv*:2206.08515 (2022).
- [47] Limei Wang et al. "Learning Hierarchical Protein Representations via Complete 3D Graph Networks". In: *The Eleventh International Conference on Learning Representations*. 2023.
- [48] Zeyuan Wang et al. "Multi-level Protein Structure Pre-training via Prompt Learning". In: *The Eleventh International Conference on Learning Representations*.
- [49] Edwin C Webb et al. Enzyme nomenclature 1992. Recommendations of the Nomenclature Committee of the International Union of Biochemistry and Molecular Biology on the Nomenclature and Classification of Enzymes. Ed. 6. Academic Press, 1992.

- [50] Fang Wu, Dragomir Radev, and Jinbo Xu. "When Geometric Deep Learning Meets Pretrained Protein Language Models". In: *bioRxiv* (2023), pp. 2023–01.
- [51] Gang Xu, Qinghua Wang, and Jianpeng Ma. "OPUS-Rota4: a gradient-based protein side-chain modeling framework assisted by deep learning-based predictors". In: *Briefings in Bioinformatics* 23.1 (2022), bbab529.
- [52] Jianyi Yang et al. "Improved protein structure prediction using predicted interresidue orientations". In: Proceedings of the National Academy of Sciences 117.3 (2020), pp. 1496–1503.
- [53] Zuobai Zhang et al. "Protein representation learning by geometric structure pretraining". In: *International Conference on Learning Representations*. 2023.

A Appendix

A.1 SE(3)

The collection of 4×4 real matrices of the SE(3) is shown as:

$$\begin{bmatrix} R & \mathbf{t} \\ 0 & 1 \end{bmatrix} = \begin{bmatrix} r_{11} & r_{12} & r_{13} & t_1 \\ r_{21} & r_{22} & r_{23} & t_2 \\ r_{31} & r_{32} & r_{33} & t_3 \\ 0 & 0 & 0 & 1 \end{bmatrix},$$
(11)

where $R \in SO(3)$ and $\mathbf{t} \in \mathbb{R}^3$, SO(3) is the 3D rotation group. R satisfying $R^TR = I$ and det(R) = 1.

A.2 Details of Model Architecture

As stated in Sec. 3.3 on sequence-structure graph convolution, l is set to be a constant number 11. We increase the predefined radius r to 2r after one pooling layer, and the number of feature channels for node embeddings is also doubled. We use a Leaky ReLU function [13] as the activation $\sigma(\cdot)$ in the message passing layers.

We design the sequential and radius graph instead of the k-nearest neighbour graph because a constant k make some neighbor nodes far away from the center node. As shown in Figure 7, the distances of a group of neighbor nodes ($\|P_{i,C\alpha}-P_{j,C\alpha}\|$) are larger than 20 Å, which cannot be seen as contacts [9]. Therefore, the radius is initially set to 4, enlarging to 16 in deeper layers. There are four massage passing and pooling layers. In this condition, when the number of nodes decreases, l is constant, r increases, neighbours of center nodes gradually cover more distant nodes.

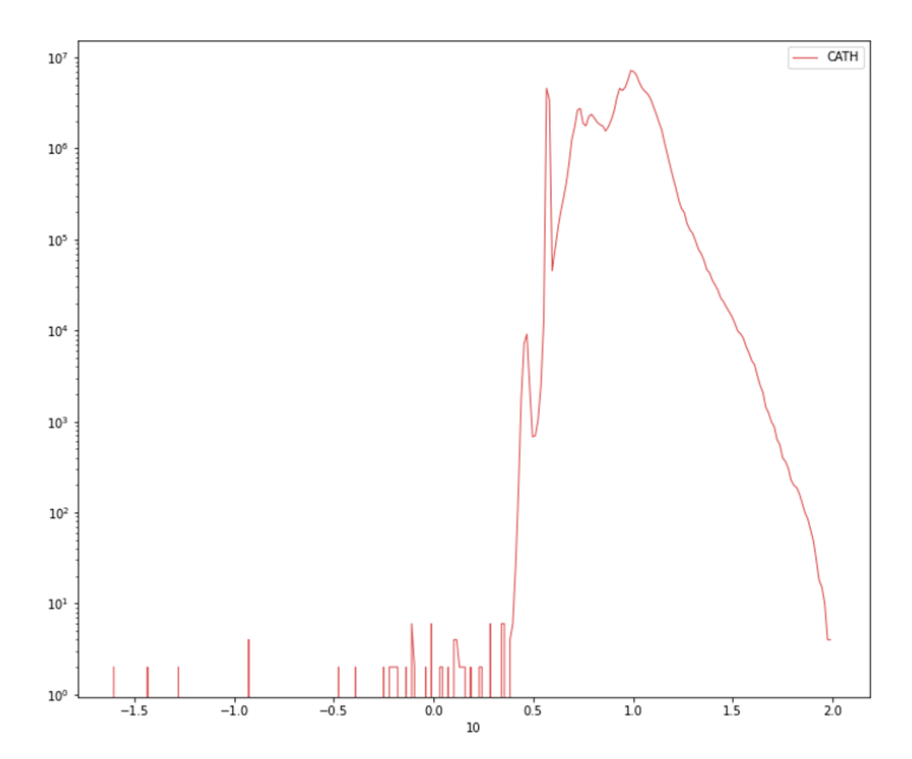


Figure 7: The histogram of distance statistics of k=30 nearest neighbor nodes of a protein dataset (CATH [29]). The horizontal axis denotes the distance in terms of exponents of 10, and the vertical axis represents the number of neighbor nodes with this distance.

Table 4: Dataset statistics. # X means the number of X.

Dataset	# Train	# Validation	# Test
Enzyme Commission	15,550	1,729	1,919
Gene Ontology	29,898	3,322	3,415
Fold Classification - Fold	12,312	736	718
Fold Classification - Superfamily	12,312	736	1,254
Fold Classification - Family	12,312	736	1,272
Reaction Classification	29,215	2,562	5,651

A.3 Details of Datasets and Training Setup

For all datasets, we use a data augmentation strategy by adding noise for the training set to increase the variability of data. For example, we update the position of $C_{\alpha i}$,

$$P_{i,C_{\alpha}} \leftarrow P_{i,C_{\alpha}} + N(\mu_N, \sigma_N^2) \tag{12}$$

where μ_N , σ_N^2 are the mean (expectation) and variance of the normal distribution N, which are set to 0 and 0.1 in experiments. Dataset statistics [53] of our four downstream tasks are summarized in Table 4.

Settings The proposed models are conducted on a single NVIDIA-SMI A100 GPU, through PyTorch 1.13+cu117 and PyTorch Geometric 2.3.1 with CUDA 11.2. The number of the initial feature channels is 256. The learning rate is set to 0.001. More details about implementation is shown in Table 5.

Table 5: More details of training setup

Tueste et training settep							
Hyper-parameter	Fold	Enzyme Reaction	GO	EC			
Batch size	4	4	24	64			
Epoch	400	400	500	500			

A.4 Evaluation Metric $F_{\rm max}$

 F_{max} is calculated by first determining the precision and recall for each protein, then averaging these results over all proteins [53, 15, 19]. p_i^j is the prediction probability for the j-th class of the i-th protein, given the decision threshold $t \in [0, 1]$, the precision and call are give as:

$$\mathrm{precision}_i(t) = \frac{\sum_j \mathbb{I}[\left(\left(p_i^j \geq t\right) \cap b_i^j\right)]}{\sum_j \mathbb{I}[\left(p_i^j \geq t\right)]}, \quad \mathrm{recall}_i(t) = \frac{\sum_j \mathbb{I}[\left(\left(p_i^j \geq t\right) \cap b_i^j\right)]}{\sum_j b_i^j}$$

where $b_i^j \in \{0,1\}$ is the corresponding binary class label, and $\mathbb{I} \in \{0,1\}$ is an indicator function. If there are N proteins in total, then the average precision and recall are defined as:

$$\operatorname{precision}(t) = \frac{\sum_{i}^{N} \operatorname{precision}_{i}(t)}{\sum_{i}^{N} \left(\left(\sum_{j} \left(p_{i}^{j} \geq t \right) \right) \geq 1 \right)}, \quad \operatorname{recall}(t) = \frac{\sum_{i}^{N} \operatorname{recall}_{i}(t)}{N}$$

Finally, $F_{\rm max}$ is defined as the maximum value of F-score over all thresholds,

$$F_{\text{max}} = \max_{t} \left\{ \frac{2 \cdot \operatorname{precision}(t) \cdot \operatorname{recall}(t)}{\operatorname{precision}(t) + \operatorname{recall}(t)} \right\}$$
(13)

A.5 More Results of GO Term Prediction

For GO term prediction, we also apply different cutoff splits. Proteins in the test set are categorized into five groups based on their similarity to the training set (30%, 40%, 50%, 70%, and 95%). As

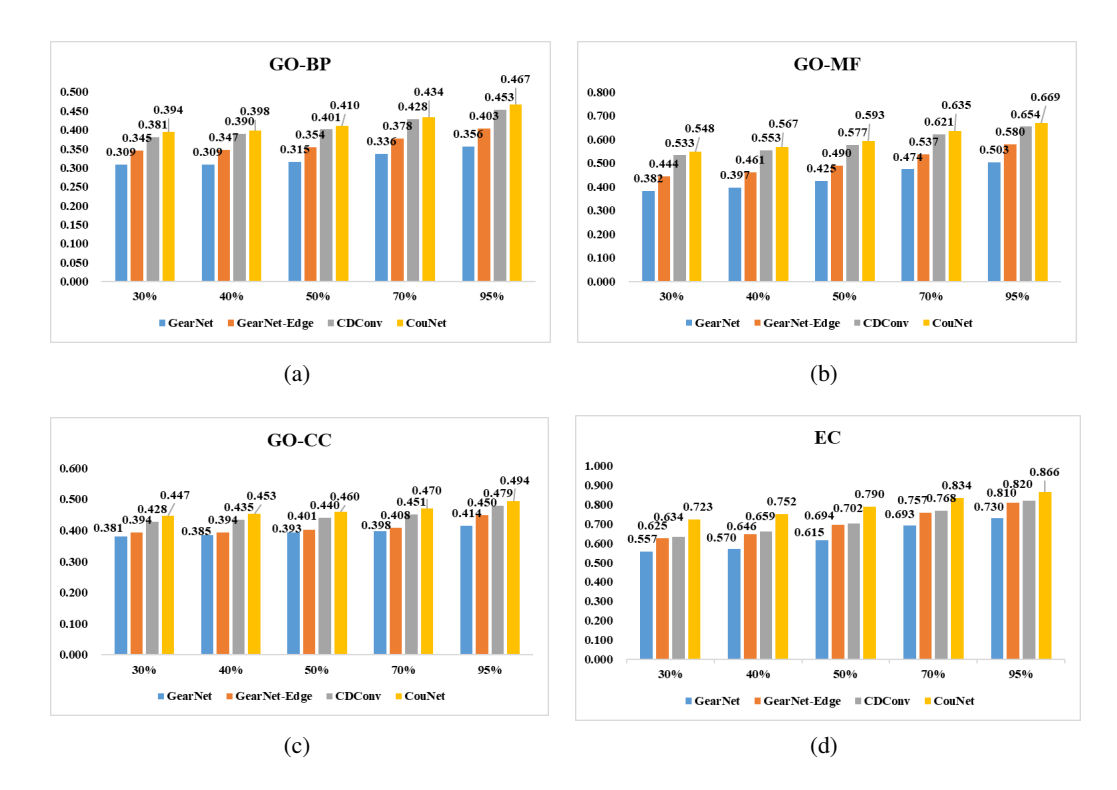


Figure 8: $F_{\rm max}$ on GO term and EC number prediction under different cutoffs.

shown in Figure 6, the results of GO term prediction are presented in Figure 8(a)-(c). The proposed model CoupleNet achieves the highest $F_{\rm max}$ scores across all cutoffs on these tasks. Even when there is a low similarity between the training and test sets, our model also has higher scores, which demonstrates the superiority and robustness of the proposed model.

A.6 Completeness Analysis

Given a protein 3D graph $G=(\mathcal{V},\mathcal{E},\mathcal{P})$, we capture the geometric representations based on the atoms' 3D positions and use sequential and structural representations as the node and edge features. For a 3D structure, based on the definition of completeness in Sec. 3.1 and the rigorously demonstrated method to show the calculated geometries can achieve completeness for structures [47], we guarantee the completeness of the selected geometric representations at the base and backbone levels of structures.

The geometric representations are SE(3) invariant (distances, angles) and SE(3) equivariant (directions, orientations). Therefore, it is natural for Eq. 3 to hold from right to left. To demonstrate Eq. 3 holding from left to right, we need to show $\mathcal{F}(G) \Rightarrow T_g(\mathcal{P})$, where T_g does not change the 3D conformation of a 3D graph. Thus we need to show positions can be determined by $\mathcal{F}(G)$.

The base approach CoupleNet_{aa} only considers the C_{α} coordinates and constructs LCS for each residue. $\mathcal{F}(G)_{aa}$ provides complete representations. First, when n=1, it holds. Assume the case n=k holds such that $\mathcal{F}(G)_{aa}$ is complete. Then we need to prove the case n=k+1 still holds. This is obvious because if v_j is the (k+1)-th node connected to node v_i among the existing k nodes, the LCS Q_j can be easily obtained from Q_i and $\mathcal{F}(G)_{aa}$.

Table 6: More Ablation of our proposed method

Method	Fold Classification		Enzyme	GO		EC		
1,10,110,0	Fold	Superfamily	Family	Reaction	BP	MF	CC	20
CoupleNet w/o sequence w/o structure	60.6 60.0 26.1	82.1 81.6 36.4	99.7 99.6 92.9	89.0 88.4 81.3	0.467 0.441 0.406	0.669 0.650 0.586	0.494 0.456 0.427	0.866 0.700 0.625

A.7 More Results of Ablation Study

Table 3 presents an ablation study of the proposed CoupleNet model. Apart from removing Φ, Ψ, Ω or $d, \omega, \theta, \varphi$ and using the base model CoupleNet_{aa}. we conduct more ablation experiments on the four tasks. The results are shown in Table 6.

Compared with the full model, we consider removing either the sequence or structure information to analyze their importance. Removing the sequence information means removing the encoding of amino acid types for each node. Removing the structure information means removing features related to protein geometry $(\mathcal{F}(G)_{aa}, \Phi, \Psi, \Omega, d, \omega, \theta, \varphi)$, and we omit related subscripts for brevity).

As shown in Table 6, removing either sequence or structure causes a performance drop on all tasks, demonstrating that both types of information are critical for the proposed method. When removing the structure, the performance decreases more significantly, suggesting that structural information provides more important and comprehensive clues compared with sequence information alone. Combining these diverse data sources leads to optimal predictive performance.